2018 IEEE International Conference on Soft Robotics (RoboSoft)
Livorno, Italy, April 24-28, 2018

A Soft Robotic Exo-Sheath using Fabric EMG Sensing for Hand Rehabilitation and Assistance

Jiaqi Guo, Shuangyue Yu, Yanjun Li, Tzu-Hao Huang, Junlin Wang, Brian Lynn, Jeremy Fidock, Chien-Lung Shen, Dylan Edwards, and Hao Su*

Abstract— **This paper presents the design and evaluation of a soft hand exo-sheath integrated with a soft fabric electromyography (EMG) sensor for rehabilitation and activities of daily living (ADL) assistance of stroke and spinal cord injury (SCI) patients. This wearable robot addresses the limitations of the soft robot gloves with design considerations in terms of ergonomics and clinical practice. Its features include: this exo-sheath is based on electric actuation and has been designed to be compact and portable. It reduces the shear force and avoids kinematic singularity comparing with tendon-driven soft gloves as their tendon routings are typically in parallel with individual fingers. Disparate from conventional robotic gloves, this design optimizes a bio-inspired fin-ray structure to enhance the hand proprioception as the palm is not covered by wearable structures. With a novel self-fastening finger clasp design, wearers can self-don/doff the exoskeleton device simplifying ADL assistance. To develop more intuitive control interface, a soft fabric EMG sensor has been developed to understand human intentions. The functionality of this soft robot has been demonstrated with experimental results using the low-level position control, kinematics evaluation and reliable EMG measurements.**

I. Introduction

The human hand is one of the most complicated products of evolution. In rehabilitation science, hand rehabilitation plays a critical and unique role for neural plasticity which provides a foundation for recovery of motor function after stroke and spinal cord injury (SCI). In the meanwhile, hand rehabilitation is formidably challenging due to the complexity of sensorimotor control required for hand function as well as the wide range of recovery of manipulation abilities.

The wearable robotics research is going through several key paradigm shifts. One trend is to develop robots to support the movement generation in joint space instead of supporting the resultant movement in task space. The early pioneering work in this field typically fall into the second category. The task-space type robots assist the distal portion of the users (the end-effector using the robotics terminology), such as MIT MANUS [1], Mirror Image Movement Enabler (MIME) robotic device [2], and Amadeo robotic system [3]. It typically has relatively simple mechanism and less degrees of freedom (DOF) than the DOF in joint space. It is primarily developed for rehabilitation applications and typically fixed on a base platform and not wearable. The joint-space type robots assist users in the anthropomorphic joint space providing natural movement, e.g. the upper limb exoskeletons by Kim et al. [4] for shoulder joint and Gijbels et al. [5] for the upper limbs. Those are typically wearable robots that have articulated structure and the same DOF with its biological counterparts.

Another trend in rehabilitation robots is to shift from the bulky and rigid design to soft or hybrid rigid/soft design. Compared with traditional design with rigid structures, soft robotics has demonstrated its potential due to its comfort human-robot interaction and its capability to interact with environment with unknown properties. Soft wearable robots typically consist of three key sub-system: actuation unit, transmission unit and wearable unit.

In terms of actuation approaches, soft hand exoskeletons can be classified into two main categories: pneumatic and electrical actuations. Pneumatics actuated hand orthoses, represented by the Harvard soft robot glove Polygerinos et al. [6], [7] and National University of Singapore pneumatic soft glove [8][9], are typically not portable as it requires cumbersome and bulky air pump. In terms of electrical actuation, Jeong et al. and Kang et al. exploited a bio-inspired soft tendon-driven system Exo-Glove Poly [10]–[14], that leverages silicone as the material for wearable structure design to maintain hygiene and washability. Xiloyannis et al. [15] developed the tendon-driven robotic glove, using Bowden cable transmission and brushless motor actuator to under actuate 8 DOF. Researchers from the Bioservo Technologies AB [8], [16] designed the textile based SEM glove.

There is a strong unmet clinical need to develop hand orthoses with both robotics and clinical considerations, such as for spinal cord injury, stroke and elderly assistive [17][18][19]. First, it is desirable to be compact and portable, thus the wearers can use it both as rehabilitation and assistive devices. Second, to enhance acceptance rates, it is crucial to optimize the comfort. Tendon-driven hand orthoses typically suffer from kinematics singularity and applies significant portion of shear forces. Third, the user palms desires minimal coverage to maintain proprioception of the patients. Fourth, users prefer the exoskeleton that has self-dressing capability, and does not require assistance from others.

Besides those electromechanical requirements, an intuitive user interface that detects human intention can significantly simplify the device operation. Prior studies integrated the electrodes into the apparel to measure the human physiology signals, such as cardiopulmonary monitoring [20]–[22], ECG

Jiaqi Guo, Shuangyue Yu, Tzu-Hao Huang, Junlin Wang, Yanjun Li, Brian Lyn and Hao Su are with the Biomechatronics and Intelligent Robotics Lab, Department of Mechanical Engineering, City University of New York, City College, NY, USA. *Corresponding author: hao.su@ccny.cuny.edu

Chien-Lung Shen is with the Taiwan Textile Research Institute, Taiwan, Republic of China.

Jeremy Fidock and Dylan Edwards are with the Department of Neurology, Weill Cornell Medicine, Cornell University, NY, USA.

sensing by the conductive yarn [20], [21], motion sensing by the piezo-resistive yarn [23], [24] and electromyography (EMG) measurement [25]–[27]. Our method is knitting-based as it is and more comfortable than embroidery or woven methods.

In this paper, we exploited a soft under-actuated hand exoskeleton integrated with a fabric sEMG interface[28], [29], as shown in Fig. 1. The system has two DOF on each finger (flexion and extension) and can be used for both rehabilitation and home-assistance purposes. Unlike traditional pulley system used in most motor-actuated designs, a bioinspired fin-ray structure [28], [29] is adapted to reduce weight and size in transmission and achieve a portable, compact system with optimized force transmission structure that could reduce shear force on fingers and improve user experience.

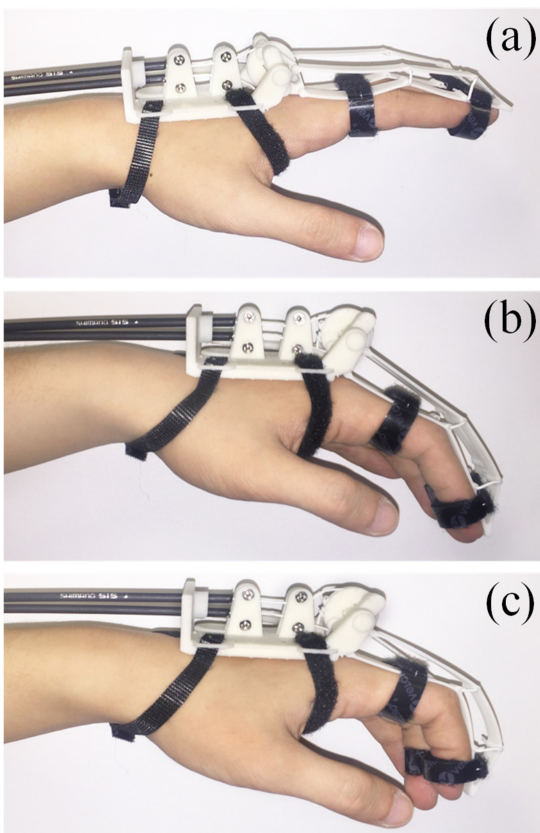

Fig. 1. Soft bidirectional tendon-driven hand exoskeleton is lightweight and assists both hand flexion and extension. It has the potential to be used for both stroke and SCI patients. (a) shows the hand extension posture with exoskeleton assistance to improve hand function of stroke patients. (b) is the neutral posture. (c) shows the hand flexion posture with exoskeleton assistance to improve hand function of SCI patients.

II. Design Requirements

In a nutshell, a soft robotic exoskeleton that augment or restore hand function for stroke and SCI patients both in rehabilitation procedures and daily activities is desirable. Soft robot glove using cable-driven transmission (e.g. the Exo-Glove Poly) suffer from significant amount of shear force in patients' fingers, leading to unpleasant user experience. Our propose an adaptive fin-ray [30], [31] based design to reduce shear force and achieve better transmission structure. Using the structure, one actuator under-actuates the metacarpophalangeal (MCP), peripheral interphalangeal (PIP) and distal interphalangeal (DIP) joints flexion-extension. A fabric sEMG interface has been developed and its output data was analyzed by a classifier to detect and understand patients' intention. Detailed design requirements of kinematics and kinetics parameters is shown in Table 1.

A. Kinetics Requirement

As stated before, the soft exo-glove is designed to help with both rehabilitation and activities of daily living (ADLs), thus, it is important to study patients' hand biomechanics and understand how much strength is needed to perform ADLs. The amount of strength stroke or SCI patients can voluntarily grip is often viewed as a measurement of hand function. According to studies in [8], [11], [14], [32], albeit patients' grip force shows great variance (18N ±27 N), the worst case (patients with no grip strength) is chosen as our force output design requirement such that the robotic exo-glove could meet the demand of all other cases in both rehabilitation and ADLs situations.

Cable-driven transmission for soft robot glove design [33]–[35] has been explored to drive patients' fingers to perform flexion and extension. In such structure, cable is attached to the surface of fingers and pulls each finger knot to rotate around the joint accordingly. The major drawback of traditional cable-driven system causes significant amount of shear force applied on patients' fingers and results in an unpleasant user experience.

B. Kinematics Requirement

In rehabilitation procedures, patients are asked to perform various hand motions according to instructions from rehabilitation or medical devices [36]. Instead of accurate and powerful grasp of weighted objects, the initial phase of rehabilitation requires merely simple motions of hand such as flexion and extension of individual finger. Therefore, force output strong enough to drive fingers is sufficient for rehabilitation procedures. As for activities of daily living, this paper focuses on three main tasks that would be performed several times every day by healthy people, namely typing with a keyboard, holding a bottle, and opening a door with knob handle. The maximum value of ROM (range of motion) and force among these activities is chosen as design criteria of the hand exoskeleton.

This paper explores the fin-ray structure as force transmission device on fingers. However, unlike its implementation in Festo Adaptive Gripper, the fin-ray structure must be adjusted to fit human hand curvature as initial states of human fingers of both healthy people and stroke or SCI patients are not straight. In this paper, curvature of seven hands from different people are studied to find an averaged initial state. Experimental objects are required to sit still and place their hands on a horizontal plane and stay relaxed. Further, they are required to hold items mentioned in the last paragraph with normal force and lift them up in the air. We took pictures of their hands in both relaxed or grasping states, and manually marked finger joints and phalanges in MATLAB math work 2017b[8]. The data is used to generate kinematics parameters later in our analysis.

C. Intelligent System & Intention Detection Requirement

To help patients in their ADLs, the exo-glove system is required to have the ability to detect patients' intention actively. In Nilsson's design [14], pressure sensors are attached to each finger tip, and the system provides users with hand strength proportional to the feedback of the pressure sensors. And in Exo-Glove Poly [37], an analog switch is the only input to control flexion and extension. In this paper, we propose a soft sEMG interface that is wearable on patients' arm to detect patients' arm motion. And a SVM classifier trained on data collected from the sEMG to understand patients' intention.

TABLE I. COMPARISON OF DESIGN REQUIREMENT FOR REHABILITATION AND ASSISTANCE PURPOSES

Parameters	Rehabilitation	Assistance
Weight (g)	500	300
Actuated DOF	1	1
Size (mm^3)	154 × 40 × 14	154 × 40 × 14
Distal phalange ROM (deg)	+10 ~ -145	+5~ -100
Metacarpal ROM (deg)	+10 ~ -30	+5 ~ -45
Grip Force (N)	N/A	35
Intention Detection	N/A	sEMG

III. SYSTEM DESIGN

According to the design requirements, this paper presents the detailed system design and construction procedures in the following sections: actuation and transmission design, wearability design, electronics design, and sEMG interface design.

A. Actuation & Transmission Design

As shown in Fig. 2 (a), the entire mechanical transmission system is a combination of Bowden cables, pulleys and grippers. The flexible grippers can keep a tight fit and comfortable interaction with the fingers. This system also allows bidirectional and long-distance transmission of the assistive power to human fingers, so it is not necessary to mount the heavy electric motor close to the fingers. As a result, the system on the back of the hand can be simple and light. The Bowden cable can remotely transfer the output power of the motor to the pulley fixed on the support pad (pulley1). Then, pulley1 further transfers the power to two fin-ray grippers with a shaft, driving the grippers to provide required forces and help patients extend or flex their index and middle fingers.

We select Faulhaber's DC motor 2232U012SR as the actuator of our system. Integrated with a gear reducer, the DC motor can generate torque up to 1Nm and maintains good backdrivability. The output shaft of the motor and the axle hole of a pulley (pulley2) form an interference fit, so the pulley can rotate together with the motor shaft and drive the cables.

The Bowden cable system includes cables, cable sheaths and cable mounts. This system can provide a steady bidirectional transmission process even when the hand is moving. With sheaths outside, Bowden cable can keep a constant length between cable mounts, so it will not become slack compared with no sheath condition. This characteristic gives Bowden cables the unique ability to transmit power with the movement of the hand. However, because of the stiffness, it is hard to loop the conventional steel Bowden cables over our small pullies. To solve this problem, we adopt thin Vectran lines to replace steel cables for receiving or outputting torque. To allow the cable system to transmit bidirectional forces, a pulley drives or is driven by two cables in our design. The ends of the two cables are put in the hole on the surface of the pulley groove, with two large knots which avoid themselves escaping from the hole. Regardless of the direction of the rotation, pulley2 will always pull one of the cables. Therefore, this design endows our cable system with the ability to apply bidirectional forces.

Due to the versatility and the simplicity in designing and manufacturing, we employ pulley1, a shaft and two small links to apply torques on the two fin-ray grippers. This mechanism provides the grippers with a sufficient region of motion to help patients flex or extend their fingers, while the uncomfortable sliding motion and shear forces between the grippers and the fingers is kept in a low level. With the mate between the square hole of Pulley1 and the rectangular shaft, Pulley1 can drive the shaft without extra complex structures. Similarly, two small links with rectangular holes can rotate together with the shaft and drive the grippers to pull or push the fingers. As described above, we use two cables to drive pulley1, which means pulley1 can rotate around half of a circle from the initial position (the initial position is the point where the system keeps the fin-ray grippers vertical). To reduce the sliding motion between the bottom surface of the fin-ray grippers and the upper surface of fingers, we adopt two design principles. The first principle is reducing the radius of pulley1, and the second one is reducing the distance between the shaft and the fingers as much as possible. Because of keeping the center of rotation close to the fingers, such design can largely eliminate the discomfort resulted from the shear force. The components on the back of the hand are mounted on a stable support pad, whose bottom surface is designed to fit the dorsal surface of the hand, while the upper surface is flat. The support pad is fixed with the hand by four Hook and Loop fastening straps. Fig. 2 (b) shows the exploded view of these parts.

In this paper, we modified the fin-ray structure to such that the shear force between fingers and grippers can be further reduced. The fin-ray effect, first discovered by Leif Kniese in 1997, describes a flexible structure to transmit forces. Inspired by rays of fins, the fin-ray structure consists of two cartilaginous longitudinal rays that are attached to each other at either side and connected in the middle by separated elastic tissue. When forces are loaded on either side of the rays, the overall structure bends towards the direction of the load. The technical design in some researches like the Festo Adaptive Gripper is simple: an actuate-angled triangle with flexible sides stands as the basic element, and articulated braces are connected to both sides and keep them apart. When there is no load on the system, the two sides of the triangle remain straight. However, this initial state does not fit the curve of relaxed human hands. In our studies, we viewed the fin-ray structure as two connected four-bar linkage mechanisms to simplify kinematics analysis, and the layout of connective braces and the length of each side in the linkage are modified to fit human hand biomechanics.

With the simplification of the gripper to a linkage system, we analyzed the kinematics of the gripper. The entire transmission system has three degrees of freedom (DOF). Because the distance of AB is invariant during the motion, the constraint equation of the four-bar linkage ABCD is:

$$\left(\overline{CD}+\overline{DB}-\overline{CA}\right)\bullet\left(\overline{CD}+\overline{DB}-\overline{CA}\right)=c^2 \tag{1}$$

After expanding Eq. (1), the relationship between α and β1 in Fig. 3 can be describe as:

$$2fg\cos\alpha=2cg\cos\beta_1-2cf\cos(\beta_1-\alpha)+c^2-e^2+f^2+g^2 \tag{2}$$

Similarly, γ can be determined once β1+β2 is known:

$$\begin{aligned}2ad\cos\gamma=&2cd\cos\left(\beta_1+\beta_2\right)-2ac\cos(\beta_1+\beta_2-\gamma)\\&+a^2-b^2+c^2+d^2\end{aligned} \tag{3}$$

where a, b, c, d, e, f and g are the lengths of the links.

With the 3D printing technology, we realized a rapid prototype development of our actuation system. This method allows us to design multi-functional parts with complex features, and manufacture or assemble them in a short time. The obtained parts are not only light but also strong. Except for the cables, we printed all of the components in our actuation system by Form 2, a 3D Printer produced by Formlabs. It took about four hours to print these parts in Photopolymer Resin material.

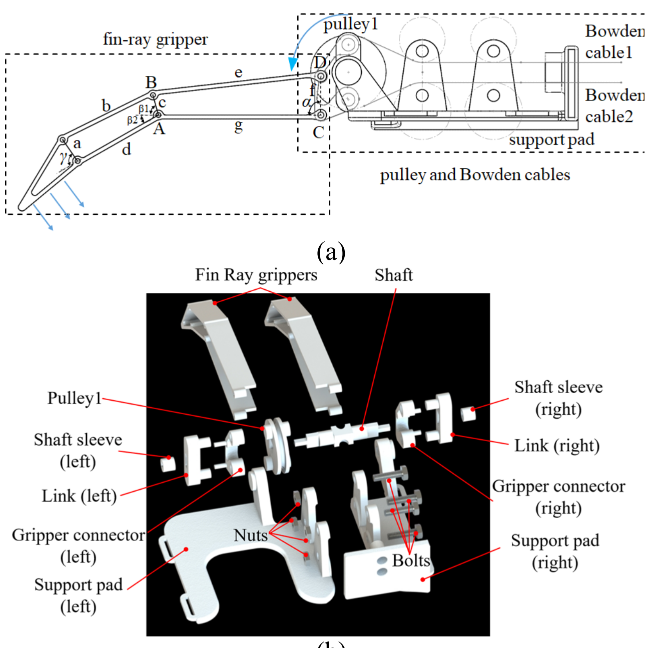

Fig. 2. Tendon-driven transmission and soft fin-ray wearable structure mechanisms design. (a) Schematic diagram of the transmission system. (b) Exploded view of components. The transmission system consists of bio-inspired fin-ray gripper, pulleys and Bowden cable system. The grippers are feasible and capable of fitting tightly with the fingers, while the shear force in the human-exoskeleton during pull and push can be kept in a reasonable level. The pulleys and Bowden cables can steadily transmit bidirectional torque to the gripper. All these components are mounted on a support pad with two parts connected by bolts and nuts. For simplification, the remotely mounted electric motor and the pulley2 connected with it are not shown in this figure.

B. Self-Fastening Finger Clasp

The design of the exo-glove necessitates a flexible mechanism to connect the transmission to the human hand. The patient must be able to mount the exo-glove with no assistance from another person, and fully flex his or her finger. The mechanism must be able to remain in place despite distal and proximal forces applied to the mechanism, and transmit flexion and extension forces to the finger.

The design of this mechanism, the finger clasp, is modeled after the medical finger trap used in closed fracture-reduction procedures. The interwoven mesh allows a finger to slide into the clasp with only a proximal force applied to the end, seen in Fig. 3 (a) to (b). The mesh locks the finger in place when a distal force is applied to the clasp, seen in Fig. 3 (c). The distal end of the finger clasp is capped to prevent proximal translation of the clasp. To release, a distal force is applied to the proximal end of the clasp.

The finger clasp is 3D printed using elastic thermoplastic polyurethane filament. This inexpensive material has a shore hardness of 85A, allows 660% maximum elongation, is chemical resistant, and does not dissolve in or absorb water. This method also allows each clasp to be fabricated to custom dimensions for the best fit.

The primary feature of the self-fastening finger clasp is the patient's ability to don and doff the device without assistance. Secondly, the clasp allows for flexion of the finger with no restriction. Thirdly, the clasp does not cover the palm, allowing the skin to breathe. Lastly, the clasp is inexpensive, robust, and versatile.

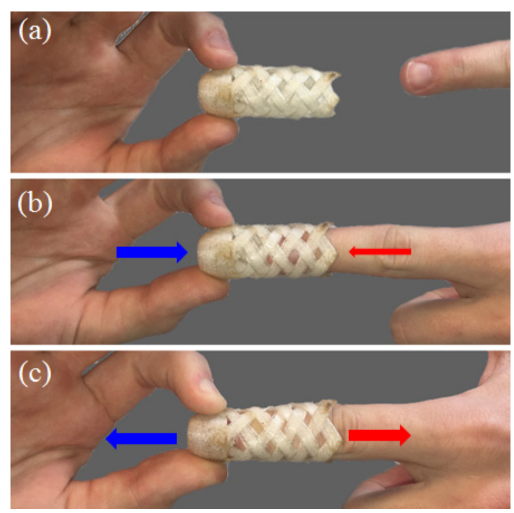

Fig. 3. Self-fastening finger clasp. (a) The initial status of finger clasp. (b) While putting on the clasp, assistive hand pushes the clasp to the finger. Blue arrow denotes the direction of force from the assistive hand, and red arrow denotes the friction from the finger. Notice the friction is relatively small because the mesh is loose. (c) If the clasp is pulled by the tip, denoted by the blue arrow, the mesh on the finger will be fastened, and thus generates a large opposite force, denoted by the red arrow, to hold the clasp on the finger.

C. Soft Fabric sEMG Sensor

A fabric-based soft wearable system that can be comfortably worn by users has been designed to detect sEMG signal, as shown in Fig. 4(a). It can be used to detect patients' movement intention and help to realize his/her fingers flexion/extension. The wearable sEMG detection system mainly consists of wearable electrodes and signal processing board.

For the measurement of the EMG signal, the silver knitting fabric electrode with low resistance was designed. The property of the silver yarn is shown in Table II. The resistance of 10-centimetre interval of fabric electrode is tested and there are three kinds of conditions for testing, 1. Measure the resistance of dry electrode directly; 2. Measure the resistance after putting fabric electrode into acid liquid 24 hours and placing in the shade to dry; 3. Measure the resistance after putting fabric electrode into alkali liquid 24 hours and placing in the shade to dry according to ISO105-E04. The results showed the maximum resistance is below 16.8Ω in all testing and the resistance was low enough for measuring the EMG signal.

TABLE II. THE RESISTANCE OF CONDUCT FABRIC AFTER ACID AND ALKALI PROCESSING, DEMONSTRAING ITS FEASIBILITY TO BE USED IN CONTACT WITH HUMAN SKIN WITH SIMILAR ACID AND ALKALI ENVIRONMENT

Processing Method	Resistance
Dry fabric	1.2±0.1Ω
Acid liquid	14.7±2.1Ω
Alkali liquid	6.5±0.8Ω

To wear the device on the arm, the textile EMG sensor was developed, shown in Fig. 4(b). The EMG signals of antagonist's muscles are sensed by the textile sensors. Each muscle of extensor and flexor has two fabric-based electrodes to measure their muscle signal and there is one reference electrode to reduce the common mode noise. The electric contacts between the fabric-based sensor and the Bluetooth controller are achieved by metallic buttons.

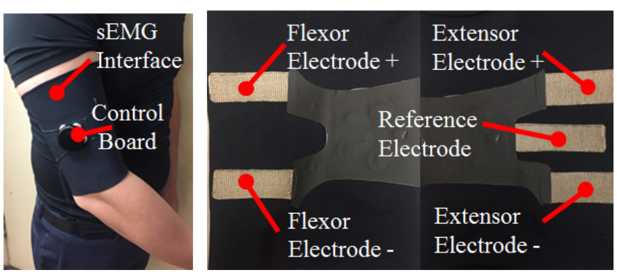

(a) (b)

Fig. 4. Configuration of wearable sEMG surface: (a) shows the wearable sEMG interface and its portable control board; (b) shows the designed wearable EMG sensors has five electrodes, two pairs of electrodes for measuring biceps and triceps muscle signal separately, another one electrode as a reference.

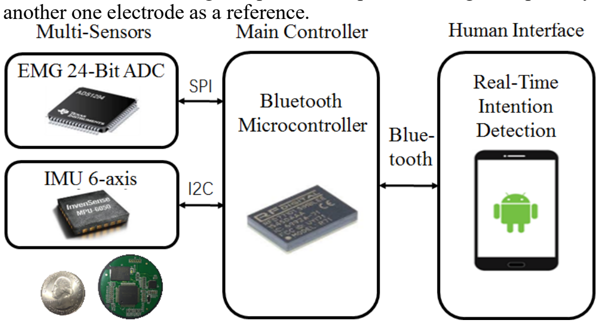

Fig. 5. The control system of the sEMG interface uses multi-sensors to detect human intention, it has features of low volume and low power consumption. The system uses Bluetooth Microcontroller (RFD77101, RF Digital, US) as the main controller to obtain and process the Semg (ADS1294, Texas Instruments, US) and IMU (MPU6050, InvenSense, US) signal. Based on data fusion and identification, the system detect human motion intention and transmitted the result to the human interface through the Bluetooth communication. Besides, the result can also be used to control out design of finger assistive and rehabilitation device.

The system board is composed of a 24-bit ADC ADS1294 (TI, Dallas, TX, USA), gyroscope & accelerometer MPU-6050 (InvenSense Inc., Sunnyvale, CA, USA), and a low-energy Bluetooth controller, shown as Fig. 7. The muscle signals are acquired by the 24-bit ADC ADS1294 and the motion signals are acquired by the 16-bit 3-axial accelerometer and 3-axial gyroscope. Those EMG and motion data are collected by the controller and sent to the cell phone by Bluetooth.

D. Electronics Design

Because our design is for both SCI and stroke patients whose hand motor function is impaired, it is important to control finger flexion/extension in a simple way. After performing usability evaluations of different sensors, including bending sensor, inertial measurement unit (IMU) and electromyography (sEMG), we find using one of sensor mentioned above individually is not satisfying the need of detecting move intention of both SCI and stroke patients. While we also find in some way, using data fusion of IMU and sEMG signal can enhance patients' finger movement intention detection effect to an acceptable level. Based on that, Fig. 6 shows the control system diagram using both IMU and sEMG to realize control feedback.

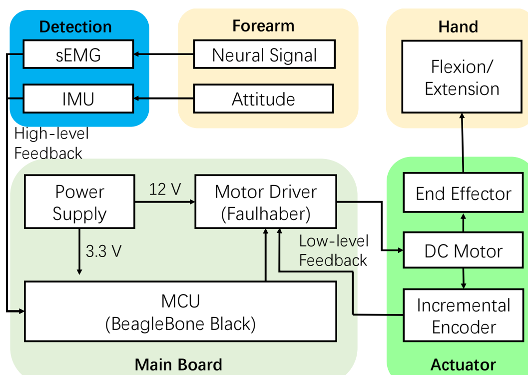

Fig. 6. The diagram shows the control system of the design. When patients want to flexion/extension their finger, the neural and muscle of his/her arm will be slightly changed. The IMU and sEMG sensor can detect the variation and send signals to the Microcontroller unit (MCU). Based on these feedback signal, MCU process the data and controls DC motor and actuate end-effector to assist finger movement.

The electronics design mainly consists of the main control board, an actuator unit, and sensor boards. A commercially available MCU (BeagleBone Black development board, Texas Instruments LLC) is used with the main control board. The board handles IMU and sEMG data acquisition through UART communication, and also handles sending a motor control command using PWM. Besides, to develop the system fast, a commercially available motor controller (MC5010S, Faulhaber LLC) located on the main board is used to realize low-level close-loop motor control. The actuator unit consists of a DC motor (12 V, 3.66W), gearbox (43:1 ratio, 3 stages planetary) and encoder (64 line, incremental). Two sensor boards are used to detect patient's movement intention, one is a commercial attitude and heading reference system, which consists of a three-axis accelerometer, a three-axis gyroscope, and a three-axis magnetometer; another is a custom-designed sEMG detection suit and will be introduced in the next chapter.

The motor controller and DC motor are powered by 12 V DC supply and the MCU and sensor boards are powered by 3.3 V.

IV. EXPERIMENTS AND PERFORMANCE EVALUATION

Two tests for the actuator and one test for soft sEMG interface will be presented in this part. Among them, the first test is to measure the position control effect of the DC motor, the second test is to figure out the relationship between motor rotation and the end-effector bending angle in different locations. These two tests verify the basic function of the actuator prototype we designed in these paper; The third test is about human wearing sEMG interface test. The flexion/extension intention can be detected by biceps and triceps sEMG signal variation through the sEMG interface.

A. Low-Level Position Control Test

The DC motor can actuate the end-effector through cable-driven and assist finger flexion/extension. Based on the current version of the mechanical structure, the range of motion of DC motor is from 0 to 130 degrees.

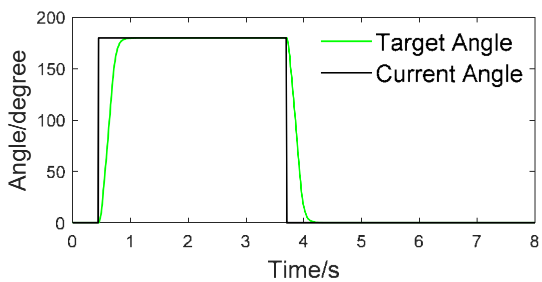

Fig. 8. DC motor low-level position control test. It shows the control result when motor rotate between 0 degrees (finger maximum extension) to 130 degrees (finger maximum flexion).

Among them, 0 degrees corresponds to maximum extension state, 130 degrees correspond to maximum flexion state. A low-level position control loop is designed and run in the motor controller, as shown in Fig. 8(a). To have a fast response to safety control effect, the position controller has a high gain factor and a -5 to 135 degrees range limits. Figure 8(b) shows the result of the step signal test. The motor takes about 0.165 s to reach 130 degrees from 0 and use about the same time to move back to 0 degrees again.

B. End-effector Flexion/Extension Test

The end-effector is fixed at the top of the finger and will assist finger flexion/extension through finger joints rotation. Due to the end-effector adopts soft design, unlike normal rigid structure, it's state of motion is hard to estimate. Thus, to realize assisting fingers flexion/extension movement, it is important to figure out the motion relationship between motor and end-effector. To measure finger joints rotation angle corresponding to DC motor position, an AHRS system (9-axis IMU sensor, HI219M, HiPNUC Technologies) has been used to measure end-effector's rotation angle variation under DC motor actuated from maximum extension to maximum flexion. As shown in Fig. 9(a), we put AHRS system in six locations to test the end-effector rotation angle when it is actuated to assist finger flexion/extension.

A 25-years old healthy man participated in this test who is about 183cm high and 80kg weight. He wears the end-effector with the index finger. His hand is fixed in the same location during the time of the whole test. The test repeats six times that the AHRS system is fixed in different positions. During every single test, DC motor rotates from 0 degrees (maximum extension state) to 130 degrees (maximum flexion state) as the step of 13 degrees per second rotation in totally 10 seconds. The AHRS system has a working frequency of 200 Hz. We use the average of 10 measurement data (0.05 s totally) to indicate joint rotation variation at each second corresponding to DC motor position variation.

The result is shown in Fig. 9(b). With the DC motor rotate between 0 to 130 degrees, the end-effector change in shape and assist finger flexion/extension. Between finger maximum extension state to maximum flexion state, the finger dorsal side of the joints rotates 56.35 (MCP dorsal), 66.17 (PIP dorsal) and 101.74 (DIP dorsal) degrees, and the finger palmar side of the joints rotates 30.71 (MCP palmar), 75.64 (PIP palmar) and 109.11 (DIP palmar) degrees separately. Although there are certainly individual differences exists, this experiment attempts to correspond the rotation position of the motor with the angle of the end-effector to assist the finger extension/flexion, which is helpful to guide us to control the whole system and demonstrate the effectiveness of this paper mentioned end-effector structural design.

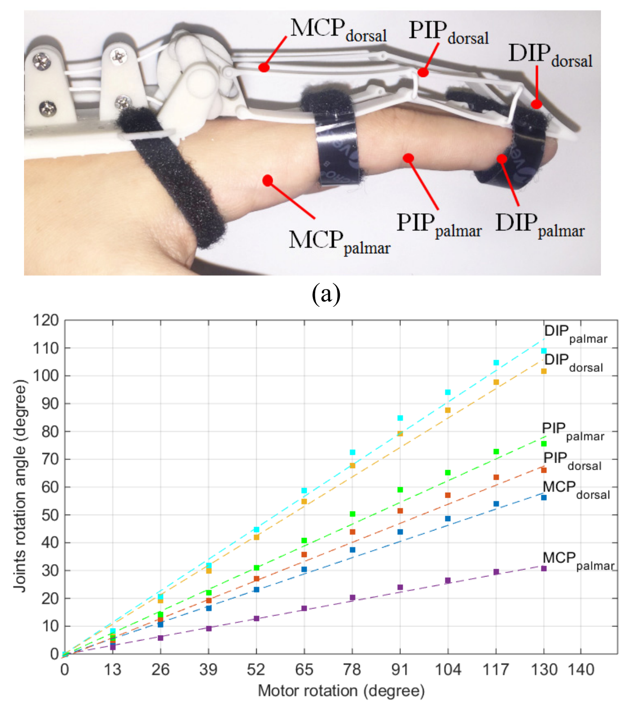

(b)

Fig. 9. Test of the end-effector flexion/extension range of motion with the DC motor rotating through 0 to 130 degrees. (a) shows the six IMU wearing fixed position, including three finger palmar side and three finger dorsal side of the actuator; (b) shows the result of testing parts' rotation variation correspond to the motor rotation between 0 (maximum extension state) to 130(maximum flexion state) degrees.

V. CONCLUSION

In this paper, we introduced a soft under-actuated hand exoskeleton which can facilitate both the rehabilitation and ADLs of stroke or SCI patients with paretic hand problems. Bio-inspired fin-ray grippers were adopted to provide patients with a soft and comfortable interface between their fingers and the exoskeleton. While simple and lightweight, our cable transmission system maintains steady and bidirectional assistance. The experiment results demonstrate the fast and accuracy tracking performance of the low-level position control system.

REFERENCES

[1] A. Hogan, N.; Krebs, H.I.; Charnnarong, J.; Srikrishna, P.; Sharon, "MIT - MANUS : A Workstation for Manual Therapy and Training I," *MIT*, pp. 161–165, 1992.

[2] P. S. Lum, C. G. Burgar, M. Van der Loos, P. C. Shor, M. Majmundar, and R. Yap, "MIME robotic device for upper-limb neurorehabilitation in subacute stroke subjects: A follow-up study," *J. Rehabil. Res. Dev.*, vol. 43, no. 5, p. 631, 2006.

[3] P. Sale, V. Lombardi, and M. Franceschini, "Hand robotics rehabilitation: Feasibility and preliminary results of a robotic treatment in patients with hemiparesis," *Stroke Res. Treat.*, 2012.

[4] B. Kim and A. D. Deshpande, "Controls for the shoulder mechanism of an upper-body exoskeleton for promoting scapulohumeral rhythm," in *IEEE International Conference on Rehabilitation Robotics*, 2015, vol. 2015–Septe, pp. 538–542.

[5] D. Gijbels, I. Lamers, L. Kerkhofs, G. Alders, E. Knippenberg, and P. Feys, "The Armeo Spring as training tool to improve upper limb functionality in multiple sclerosis: a pilot study," *J. Neuroeng. Rehabil.*, vol. 8, no. 1, p. 5, 2011.

[6] P. Polygerinos, K. C. Galloway, E. Savage, M. Herman, K. O'Donnell, and C. J. Walsh, "Soft robotic glove for hand rehabilitation and task specific training," *Proc. - IEEE Int. Conf. Robot. Autom.*, vol. 2015–June, no. June, pp. 2913–2919, 2015.

[7] P. Polygerinos, Z. Wang, K. C. Galloway, R. J. Wood, and C. J. Walsh, "Soft robotic glove for combined assistance and at-home rehabilitation," *Rob. Auton. Syst.*, vol. 73, pp. 135–143, 2015.

[8] M. Nilsson, J. Ingvast, J. Wikander, and H. Von Holst, "The Soft Extra Muscle system for improving the grasping capability in neurological rehabilitation," *2012 IEEE-EMBS Conf. Biomed. Eng. Sci. IECBES 2012*, no. December, pp. 412–417, 2012.

[9] H. K. Yap, J. H. Lim, F. Nasrallah, J. C. H. Goh, and R. C. H. Yeow, "A soft exoskeleton for hand assistive and rehabilitation application using pneumatic actuators with variable stiffness," in *Proceedings - IEEE International Conference on Robotics and Automation*, 2015, vol. 2015–June, no. June, pp. 4967–4972.

[10] D. Park, I. Koo, and K. J. Cho, "Evaluation of an improved soft meal assistive exoskeleton with an adjustable weight-bearing system for people with disability," *IEEE Int. Conf. Rehabil. Robot.*, vol. 2015–Septe, pp. 79–84, 2015.

[11] H. In, B. B. Kang, M. K. Sin, and K. J. Cho, "Exo-Glove: A wearable robot for the hand with a soft tendon routing system," *IEEE Robot. Autom. Mag.*, vol. 22, no. 1, pp. 97–105, 2015.

[12] H. In, U. Jeong, H. Lee, and K. J. Cho, "A Novel Slack-Enabling Tendon Drive That Improves Efficiency, Size, and Safety in Soft Wearable Robots," *IEEE/ASME Trans. Mechatronics*, vol. 22, no. 1, pp. 59–70, 2017.

[13] U. Jeong, H. K. In, and K. J. Cho, "Implementation of various control algorithms for hand rehabilitation exercise using wearable robotic hand," *Intell. Serv. Robot.*, vol. 6, no. 4, pp. 181–189, 2013.

[14] B. B. Kang, H. Lee, H. In, U. Jeong, J. Chung, and K. Cho, "Development of a Polymer-Based Tendon-Driven Wearable Robotic Hand," pp. 3750–3755, 2016.

[15] B. Biorob, M. Xiloyannis, L. Cappello, D. B. Khanh, S. Yen, and L. Masia, "This document is downloaded from DR-NTU , Nanyang Technological University Library , Singapore . Modelling and Design of a Synergy-based Actuator for a Tendon-driven Soft Robotic Glove based Actuator for a Tendon-driven Soft Robotic Glove . Modelling and ," 2016.

[16] B. Radder *et al.*, "User-centred input for a wearable soft-robotic glove supporting hand function in daily life," *IEEE Int. Conf. Rehabil. Robot.*, vol. 2015–Septe, pp. 502–507, 2015.

[17] Z. B. Zhang, Y. H. Shen, W. D. Wang, B. Q. Wang, and J. W. Zheng, "Design and implementation of sensing shirt for ambulatory cardiopulmonary monitoring," *J. Med. Biol. Eng.*, vol. 31, no. 3, pp. 207–216, 2011.

[18] D. S. Nichols-Larsen, P. C. Clark, A. Zeringue, A. Greenspan, and S. Blanton, "Factors influencing stroke survivors' quality of life during subacute recovery," *Stroke*, vol. 36, no. 7, pp. 1480–1484, 2005.

[19] E. Weening-Dijksterhuis, M. H. de Greef, E. J. Scherder, J. P. Slaets, and C. P. van der Schans, "Frail institutionalized older persons: A comprehensive review on physical exercise, physical fitness, activities of daily living, and quality-of-life," *Am J Phys Med Rehabil*, vol. 90, no. 2, pp. 156–168, 2011.

[20] M. Stoppa and A. Chiolerio, "Wearable electronics and smart textiles: A critical review," *Sensors (Switzerland)*, vol. 14, no. 7. pp. 11957–11992, 2014.

[21] F. Axisa, P. M. Schmitt, C. Gehin, G. Delhomme, E. McAdams, and A. Dittmar, "Flexible technologies and smart clothing for citizen medicine, home healthcare, and disease prevention," *IEEE Trans. Inf. Technol. Biomed.*, vol. 9, no. 3, pp. 325–336, 2005.

[22] J. Wang, C. C. Lin, Y. S. Yu, and T. C. Yu, "Wireless Sensor-Based Smart-Clothing Platform for ECG Monitoring," *Comput. Math. Methods Med.*, vol. 2015, 2015.

[23] A. Shafti, R. B. Ribas Manero, A. M. Borg, K. Althoefer, and M. J. Howard, "Embroidered Electromyography: A Systematic Design Guide," *IEEE Trans. Neural Syst. Rehabil. Eng.*, vol. 25, no. 9, pp. 1472–1480, 2017.

[24] T. Finni, M. Hu, P. Kettunen, T. Vilavuo, and S. Cheng, "Measurement of EMG activity with textile electrodes embedded into clothing," *Physiol. Meas.*, vol. 28, no. 11, pp. 1405–1419, 2007.

[25] X. Tao, V. Koncar, T. H. Huang, C. L. Shen, Y. C. Ko, and G. T. Jou, "How to make reliable, washable, and wearable textronic devices," *Sensors (Switzerland)*, vol. 17, no. 4, 2017.

[26] C.-L. Shen *et al.*, "Respiratory Rate Estimation by Using ECG, Impedance, and Motion Sensing in Smart Clothing," *J. Med. Biol. Eng.*, vol. 37, no. 6, pp. 826–842, 2017.

[27] C.-L. SHEN *et al.*, "SMART EMG SLEEVE FOR MUSCLE TORQUE ESTIMATION," in *Uncertainty Modelling in Knowledge Engineering and Decision Making*, pp. 549–554.

[28] O. Pfaff, S. Simeonov, I. Cirovic, and P. Stano, "Application of Fin Ray effect approach for production process automation," *Ann. DAAAM 2011 Proc. 22nd Int. DAAAM Symp.*, vol. 22, no. 1, pp. 1247–1248, 2011.

[29] S. Alben, P. G. Madden, and G. V. Lauder, "The mechanics of active fin-shape control in ray-finned fishes," *J. R. Soc. Interface*, vol. 4, no. 13, pp. 243–256, 2007.

[30] A. Sunderland, D. Tinson, L. Bradley, and R. L. Hewer, "Arm function after stroke. An evaluation of grip strength as a measure of recovery and a prognostic indicator.," *J. Neurol. Neurosurg. Psychiatry*, vol. 52, no. 11, pp. 1267–1272, 1989.

[31] C. Bütefisch, H. Hummelsheim, P. Denzler, and K. H. Mauritz, "Repetitive training of isolated movements improves the outcome of motor rehabilitation of the centrally paretic hand," *J. Neurol. Sci.*, vol. 130, no. 1, pp. 59–68, 1995.

[32] M. A. Delph, S. A. Fischer, P. W. Gauthier, C. H. M. Luna, E. A. Clancy, and G. S. Fischer, "A soft robotic exomusculature glove with integrated sEMG sensing for hand rehabilitation," *IEEE Int. Conf. Rehabil. Robot.*, 2013.

[33] A. A. Timmermans, H. A. Seelen, R. D. Willmann, and H. Kingma, "Technology-assisted training of arm-hand skills in stroke: concepts on reacquisition of motor control and therapist guidelines for rehabilitation technology design," *J. Neuroeng. Rehabil.*, vol. 6, no. 1, p. 1, 2009.

[34] D. Jack *et al.*, "Virtual Reality-Enhanced Stroke Rehabilitation," vol. 9, no. 3, pp. 308–318, 2001.

[35] H. M. Hondori, M. Khademi, L. Dodakian, S. C. Cramer, and C. V. Lopes, "A spatial augmented reality rehab system for post-stroke hand rehabilitation," *Stud. Health Technol. Inform.*, vol. 184, pp. 279–285, 2013.

[36] The Mathworks Inc., "MATLAB - MathWorks," *www.mathworks.com/products/matlab*, 2016. .

[37] G. J. Snoek, M. J. Ijzerman, H. J. Hermens, D. Maxwell, and F. Biering-Sorensen, "Survey of the needs of patients with spinal cord injury: Impact and priority for improvement in hand function in tetraplegics," *Spinal Cord*, vol. 42, no. 9, pp. 526–532, 2004.